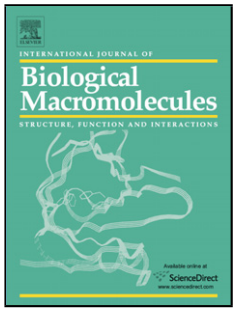

Title: Fluorescence switch biosensor based on quantum dots and gold nanoparticles for discriminative detection of lysozyme

Authors: Xuan Fu, Xing Fu, Qi Wang, Long Sheng, Xi Huang, Meihu Ma, Zhaoxia Cai

PII: S0141-8130(17)30263-5
DOI: http://dx.doi.org/doi:10.1016/j.ijbiomac.2017.05.144
Reference: BIOMAC 7633

To appear in: *International Journal of Biological Macromolecules*

Received date: 23-1-2017
Revised date: 22-5-2017
Accepted date: 23-5-2017

Please cite this article as: Xuan Fu, Xing Fu, Qi Wang, Long Sheng, Xi Huang, Meihu Ma, Zhaoxia Cai, Fluorescence switch biosensor based on quantum dots and gold nanoparticles for discriminative detection of lysozyme, International Journal of Biological Macromoleculeshttp://dx.doi.org/10.1016/j.ijbiomac.2017.05.144

Fluorescence switch biosensor based on quantum dots and gold nanoparticles for discriminative detection of lysozyme

Xuan Fu, Xing Fu, Qi Wang, Long Sheng, Xi Huang, Meihu Ma, Zhaoxia Cai*

National Research and Development Center for Egg Processing, College of Food Science and Technology, Huazhong Agricultural University, Wuhan, Hubei 430070, PR China

* Corresponding author: Zhaoxia Cai

College of Food Science and Technology of Huazhong Agricultural University, Wuhan, Hubei Province, P. R. China

Tel: +86 27 87283177

Fax: +86 27 87283177

E-mail address: caizhaoxia@mail.hzau.edu.cn

Highlights

- We report a novel strategy for lysozyme (LYZ) detection by tracing the fluorescence switch of quantum dots (QDs) and gold nanoparticles (AuNPs).

- The immune interaction between QDs-LYZ and anti-LYZ-AuNPs leads to drastic quenching (turning off) of the donor by a fluorescence resonance energy transfer (FRET) process.

- By the addition of free LYZ, anti-LYZ-AuNPs peel off from the QDs-LYZ surface and bind to free LYZ due to competitive immunoreactions, resulting in the restoration of the fluorescence intensity of QDs (turning on).

- The fluorescence intensity of the system increased linearly with increasing concentrations of LYZ from 50 to 1000 ng/mL with the detection limit of 33.43 ng/mL.

Abstract: It is important to detect lysozyme (LYZ) in a simple and rapid manner because of its potential application in the treatment of diseases and in the food industry. In this study, it was observed that the strong fluorescence of LYZ-modified Quantum Dots (QDs-LYZ) could be effectively quenched by gold nanoparticle(AuNPs) modified with antibodies against LYZ (anti-LYZ) due to fluorescence resonance energy transfer (FRET) between QDs-LYZ and anti-LYZ-AuNPs. The fluorescence can be reversibly recovered by LYZ (on state) owing to specific competitive interactions between LYZ, QDs-LYZ and anti-LYZ-AuNPs. The interaction of QDs-LYZ with anti-LYZ-AuNPs was studied by absorption, fluorescence spectroscopy and transmission electron microscopy (TEM). Under optimal conditions, LYZ can be detected with a linear range of 50 to 1000

ng/mL and a detection limit (LOD) of 33.43 ng/mL. This rapid and selective QD-based sensor was successfully applied for quantitation of LYZ in actual egg products. Furthermore, the strategy described in this report could be followed conveniently to establish similar immunosensors for the rapid detection of other proteins using corresponding antibodies.

Keywords: Lysozyme; Quantum Dots; Gold Nanoparticles; Fluorescence Switch; Anti-Lysozyme

1. Introduction

Lysozyme (LYZ), also referred to as muramidase, is a ubiquitous enzyme widely distributed in diverse organisms, such as bacteria, bacteriophages, fungi, plants and animals [1]. The primary sequence of LYZ contains 129 amino acid residues. The molecular weight is 14.3 kDa, and its isoelectric point is 11.0 [2]. LYZ is a food preservative because of its lytic activity on the cell wall of Gram-positive bacteria [3-5]. LYZ is an important defense molecule of the innate immune system, mediating protection against microbial invasion [6]. Elevated levels of LYZ in blood and urine are associated with certain diseases. LYZ has broad applications in medicine, drugs and food. Therefore, developing a rapid and sensitive method for the detection of LYZ is of great significance.

Many methods have been developed to determine LYZ, such as turbidimetric assays [7], high-performance liquid chromatography methods [8, 9] and

enzyme-linked immunosorbent assays [9]. However, a number of analytical approaches are not sufficiently sensitive, have high detection limits, or are prohibitively costly. In recent years, several methods based on spectroscopic detection were reported. Fluorescence polarization techniques and resonance Rayleigh scattering [10] have low detection limits but poor selectivity. The G-quadruplex luminescent method [11] is sensitive, but its detection range is narrow. Thus, research and utilization of LYZ methods are still limited.

Advances in nanoscience and nanotechnology have resulted in the development of various nanosensors for the detection of biomolecules. Among the nano detection techniques, optical detection has been demonstrated to be rapid and sensitive. In certain nanosensors, quantum dots (QDs) have been adopted favorably for optical detection because of the high quantum yield, good photo stability, and size-dependent tunability for the maximum emission wavelength [10, 12]. In various optical technologies, fluorescence resonance energy transfer (FRET) systems possess high sensitivity and selectivity. FRET-based studies using QDs are widely applied for DNA, bacterial and ion detection [13-15]. Using FRET technology, the fluorescence switch can be more sensitive [16, 17]. Fluorescence switching based on the FRET system perfectly combines QDs and Au nanoparticles (AuNPs), owing to the AuNPs' high extinction coefficient and broad absorption spectrum, which overlaps with the QDs' emission spectrum [18-20]. Thus, functionalized immune pairs of QDs and AuNPs could be used to establish fluorescence switching to detect LYZ.

In this work, we prepared QDs-LYZ-anti-LYZ-AuNPs nanohybrids for the

detection of LYZ using spectroscopic and fluorescence switch techniques. Two components of this immunosensor, namely, QDs-LYZ and anti-LYZ-AuNPs, were synthesized. LYZ antibody (anti-LYZ) was prepared from monospecific antiserum against lysozyme from hen egg white. As a light-absorbing material, CdTe QDs provide a "turn on" state for fluorescence measurements. This bright fluorescence is quenched in the presence of anti-LYZ-AuNPs due to the immunoreactions between LYZ and anti-LYZ ("turn off" state). After the addition of LYZ to the QDs-LYZ-anti-LYZ-AuNPs system, anti-LYZ-AuNPs become detached from the QDs-LYZ surface and attached to LYZ because of competitive immunoreactions, creating a "turn on" state. The entire assay process does not require multiple time-consuming incubations, separation and washing steps, and can be rapidly accomplished within a very short time. This fluorescence switch study will create new opportunities for engineering optically-based advanced switches for sensing biomolecules and other substances.

2. Materials and Methods

2.1 Reagents and chemicals

LYZ and avidin were purchased from Sigma-Aldrich (Louis.mo.USA). Anti-LYZ was purchased from GenWay Biotech, Inc. (Louis.Mo.USA). NaCl, KCl, NaOH, glucose, lactose, sodium citrate, Na_2HPO_4, NaH_2PO_4, $CdCl_2$, $NaBH_4$, thioglycolic acid (TGA), N-hydroxysuccinimide (NHS) and vitamin C were acquired from the Sinopharm Chemical Reagent Co., Ltd. (Shanghai, China). Glycine, cysteine,

glutathione, aspartic acid, L-serine, tyrosine, LYZ and bovine serum albumin (BSA) were purchased from the Biosharp Company (China). 1-Ethyl-3-[3-dimethylaminopropyl] carbodiimide hydrochloride (EDC) and 1-thioglycerol (TG) were acquired from the Aladdin Chemical Reagent Company Ltd. (Shanghai,China). $HAuCl_4$ was purchased from the Shanghai Chemical Reagent Company (Shanghai, China). PEG20000 was acquired from the Beijing Solarbio Science and Technology Company (Beijin,China). Te powder was acquired from the Delan Fine Chemical Reagent Company (Tianjin, China).

LYZ was prepared as a 5 mg/mL stock solution and diluted to 0.01 mg/mL as the working solution. Anti-LYZ was prepared at 5 mg/mL. All solutions were stored at 4 °C. The 0.1 mg/mL $HAuCl_4$ and 10 mg/mL sodium citrate solutions were prepared using ultra water. Phosphate-buffered solutions (PBS) with different pH values were prepared by mixing 0.01 mol/L Na_2HPO_4 and 0.01 mol/L NaH_2PO_4, according to prescribed proportions.

Egg products (egg white powder and whole egg powder) were purchased from the Kangde Biological Products Co. Ltd. (China).

2.2 Synthesis and characterization of water-soluble AuNPs

AuNPs were synthesized according to a previous report [4]. The concentration of the above AuNPs solution was 47.8 μg/mL. The solution was stored at 4 °C. A JEM-2100 transmission electron microscope (TEM) (JEOL Ltd, Japan) was used to observe the formation of AuNPs and to measure their diameters. AuNPs and the

binding products were diluted to suitable concentrations and ultrasonically dispersed for 10 min. One to two drops were placed on a copper grid, and the copper network was placed on a sample rod for TEM observations after water volatilization. The acceleration voltage was 200 kV.

2.3 Conjugation of anti-LYZ and AuNPs

Anti-LYZ (10 μg/mL) (0.05 mL) was added to 4 mL of AuNPs and later stirred for 10 min. Next, 20 μL of PEG20000 (3%, w/w) was added to stabilize the solution. After another 15 min of stirring, the solution was stored at 4 °C.

2.4 Synthesis of QDs

Thioglycollic acid-capped CdTe QDs were synthesized in an aqueous solution according to a previous report [21, 22]. First, the oxygen-free NaHTe solutions were prepared by stirring a mixture containing 36.4 mg of $NaBH_4$, 26.7 mg of Te powder and 1.5 mL of ultra water at 37 °C until the black Te powder was no longer visible. Next, 9.5617 g of $CdCl_2 \cdot 2.5H_2O$ was added to 250 mL of H_2O to form the $CdCl_2$ mother liquor. Five milliliters of the $CdCl_2$ mother liquor was diluted to 160 mL as the reaction liquid precursor. TG (140 μL) and TGA (27.5 μL) were added to the $CdCl_2$ reaction liquid precursor, followed by adjusting the pH to 11.2 by the dropwise addition of 1 mol/L NaOH. The solution was deoxygenated by purging with N_2 for 30 min. While stirring, the freshly prepared NaHTe was injected to the above solution.

The mixture was then heated to 97 °C and refluxed for 30 min. The prepared QDs solution was stored at 4 °C.

2.5 Conjugation of QDs and LYZ

Three mL of CdTe QDs was added to 2 mL of PBS (0.01 mol/L, pH 7.4), and 200 μL 4 mg/mL EDC was added to the solution to activate the carboxyl groups of the QDs. After stirring at room temperature for 5 min, the solution was incubated for an additional 15-20 min. In this process, free carboxylic acid groups on the QDs were fully activated [23]. Next, 200 μL of 0.15 mg/mL sulfo-NHS were added to the mixture and stirred for 20 min. Finally, 50 μL of 0.01 mg/mL LYZ was added to the system and reacted at 37 °C for 2 h in the dark. In this step, CdTe QDs and LYZ were conjugated through strong covalent bonds. The final bioconjugated QDs-LYZ were collected and stored in a refrigerator at 4 °C. The synthetic QDs and QDs-LYZ were characterized using TEM.

2.6 Detection of LYZ

QDs-LYZ solution (0.5 mL), 1.5 mL of anti-LYZ-AuNPs solution, 0.5 mL of 0.01 mol/L PBS, and various concentrations of LYZ (50 to 1000 ng/mL), or actual samples were added to a 10 mL tube. The mixture was diluted to 5 mL using ultrapure water and thoroughly mixed. The aqueous mixtures were incubated for 40 min at 37 °C and later cooled to room temperature. The absorption spectra of the AuNPs were obtained using a Nanodrop 2000c spectrometer (Thermo, USA). An RF-5301 spectrofluorometer (Shimadzu, Japan) was used to measure the fluorescence intensity and fluorescence spectra. The excitation wavelength was set at 330 nm. The excitation and emission slit widths were 5.0 nm. The fluorescence intensity of the binding product was recorded as F and F_0 in the presence or absence of LYZ, respectively. The change in fluorescence intensity (ΔF) was obtained by subtracting the fluorescence intensity of the binding product from that of the blank ($\Delta F=F-F_0$). The ΔF and the concentration of LYZ were used to establish a linear relationship for the quantitative detection of LYZ. The inter-particle spacing of the system was characterized using TEM images.

2.7 Sample pretreatment

Egg white powder and whole egg powder were chosen as test samples to detect the LYZ concentration because they are frequently used as raw materials in the food industry. The egg products were pretreated by centrifugation [24-25]. The sample (178.5 mg) was dissolved in 10 mL of ultrapure water. The mixtures were then centrifuged at 5000 rpm for 15 min at 4 °C to deplete the high-abundance proteins. The supernatant was collected and diluted as food samples for future detection. The concentration of LYZ in the food sample solutions was diluted until it was within the linear range of the calibration curve established in this study.

3 Results and Discussion

3.1 Scheme for the fluorescent sensor

The designed fluorescent sensor (Scheme 1) is based on the FRET between AuNPs and QDs. QDs can conjugate with LYZ under the coupling effect of EDC and NHS. QDs-LYZ indeed behaved as strong fluorescence emitters, with the monomer emission peak at 530 nm using an excitation wavelength of 330 nm. The presence of QDs-LYZ monomer produces a “turn on” state. Anti-LYZ-AuNPs binds to QDs-LYZ by recognition between LYZ and anti-LYZ under suitable pH and temperature conditions. Thus, AuNPs and QDs become close to each other, and the distance between them is less than 10 nm. One of the necessary conditions for FRET is that the distance between donor and acceptor is less than 10 nm. Thus, the electronic

excitation energy of the QDs is transferred to nearby AuNPs via a through-space dipole-dipole interaction between the QDs-AuNPs pair. Next, FRET occurs (turn off). When LYZ is added to the system, the LYZ and the QDs-LYZ in the system have the same ability to combine with the anti-LYZ-AuNPs. As the amount of LYZ in the sample is increased, the opportunity for the QDs-LYZ to combine with anti-LYZ-AuNPs is reduced, resulting in an increase in the fluorescence intensity (turn on).

3.2 Characterization of AuNPs, QDs and the binding products

The TEM images of the obtained QDs, QDs-LYZ, AuNPs, QDs-LYZ-anti-LYZ-AuNPs system, and QDs-LYZ-anti-LYZ-AuNPs system with free LYZ are shown in Fig. 1. Fig. 1A shows that the QDs were close to spherical, crystalline, sufficiently monodisperse and well-separated. The particle size of the QDs was 2.5 nm. After conjugation with LYZ, the QDs were still well-separated in the solution (Fig. 1B). This indicates that the properties of the QDs were not changed after conjugation. Thus, QDs-LYZ is suitable for subsequent use by optical detection. Fig. 1C shows that the AuNPs possessed an almost spherical morphology, and the particle size of the AuNPs was approximately 10 nm. The distance between the QDs-LYZ and the anti-LYZ-AuNPs in the QDs-LYZ-anti-LYZ-AuNPs system was less than 10 nm (Fig. 1D). A distance of less than 10 nm between the donor and the receptor is one of the necessary conditions for FRET. Thus, the short distance between QDs-LYZ and anti-LYZ-AuNPs (less than 10 nm) that resulted from the

immunological recognition of LYZ and anti-LYZ, created an essential condition for FRET. After the addition of LYZ to the QDs-LYZ-anti-LYZ-AuNPs system, LYZ and QDs-LYZ combined with anti-LYZ-AuNPs competitively through an antigen-antibody interaction (Fig. 1E). Next, the combination of QDs and AuNPs via the binding site on anti-LYZ was blocked, and a FRET between them was prohibited. The distance between QDs-LYZ and anti-LYZ-AuNPs is larger than 10 nm. Thus, FRET is blocked.

The fluorescent spectrum of QDs and QDs-LYZ is shown in Figs. 2a and 2b. The fluorescence peak for the QDs was observed at approximately 530 nm. After conjugation with LYZ, the fluorescence intensity of CdTe QDs increased slightly, and no obvious changes occurred in the fluorescent spectrum, indicating low agglomeration and fine dispersion in the labeled process [26]. UV-Vis spectra of AuNPs (Fig. 2c) indicated that the obtained AuNPs had a wide range of absorption with an absorption peak at 525 nm. According to the Beer-Lambert law, the size of the AuNPs was approximately 10 nm, which was equal to that determined from the TEM image [27]. There was a necessary overlap between the emission spectrum of the QDs (donor) and the absorption spectrum of the AuNPs (acceptor). The broad absorption of the AuNPs and the narrow emission spectra of the QDs used in this FRET laid a good foundation for energy transfer.

3.3 Optimization of the detection conditions

To obtain a high-response fluorescence sensor, experimental parameters, such as

the pH value of the solution, reaction temperature and time, were optimized (Supplemental Data Fig. S1). Considering the stability of the native structure of the LYZ, the pH value was varied from 5 to 9 for the test. The change of fluorescence intensity exhibited a trend of first rising and later falling as the pH increased from 5 to 9 and reached a maximum at pH 8 (Supplemental Data Fig. S1A). When the pH is in a neutral to an alkaline range, the QDs are stable, and it is difficult for the LYZ to bind competitively [28-29]. Moreover, a neutral pH value offers the advantage of maintaining a native conformation and biological activity and ensures the subsequent immune recognition of LYZ and anti-LYZ. Overall, a pH of 8 was chosen as the preferred reaction condition for the conjugation system.

The detection temperatures 4, 25 and 37 °C were evaluated. The maximum change of fluorescence intensity occurred at 25 °C (Supplemental Data Fig. S1B). This may be attributed to the following two points. First, a higher fluorescence intensity and better sensitivity with QDs at appropriate temperatures. When the temperature was higher than 25 °C, the change in fluorescence intensity may have declined because the QDs have a low fluorescence intensity, and the recovery of fluorescence declined at higher temperatures. Second, the maximum change of fluorescence intensity may be due to more efficient conjugation between LYZ and anti-LYZ at appropriate temperatures. Therefore, after conjugation of LYZ and anti-LYZ at 37 °C the fluorescence intensity detection temperature of 25 °C was chosen.

The fluorescence intensity of the system increased gradually as the reaction time

increased from 0 to 160 min. LYZ and QDs-LYZ competitively combined with anti-LYZ-AuNPs through antigen-antibody interactions. When the incubation time was greater than 60 min, there was no obvious increase in fluorescence intensity (Supplemental Data Fig. S1C), which implies that the reaction reached a state of equilibrium [30]. When the incubation time ranged from 60 to 160 min, the fluorescence intensity remained stable. Therefore, 60 to 160 min was chosen as the reaction times in this study.

3.4 Detection of LYZ using the fluorescence switch system

Different concentrations of the energy receptor affect the fluorescent switch system. We investigated the concentration of the energy receptor, anti-LYZ-AuNPs, in this study. As shown in Fig. 3A, after adding anti-LYZ-AuNPs to QDs-LYZ, QDs-LYZ and anti-LYZ-AuNPs were close to each other as a result of the antigen antibody interaction. The energy of the QDs-LYZ was transferred to the anti-LYZ-AuNPs. Thus, the fluorescence intensity of QDs-LYZ decreased and provided a “turn off” state. Fig. 3B shows that with an increase in the concentration of anti-LYZ-AuNPs from 0 to 25 μg/mL, the fluorescence intensity of the QDs decreased rapidly. When the concentration changed from 10-15 μg/mL, the fluorescence intensity decreased to a maximum value. Thus, 15 μg/mL anti-LYZ-AuNPs was chosen for quenching the QDs.

A calibration curve for the determination of LYZ was constructed using the optimal conditions according to the above procedures. The fluorescence spectra of the

QDs-LYZ-anti-LYZ-AuNPs system at different concentrations of LYZ are presented in Fig. 3C. With increasing concentrations of LYZ (from 50 to 1000 ng/mL), the fluorescence intensity of the system was enhanced proportionately. The probability of the combination of QDs-LYZ and anti-LYZ-AuNPs decreased as the concentration of LYZ in the samples increased. Thus, the fluorescence quenching of QDs by AuNPs was reduced. The fluorescence intensity of the system was enhanced, and the concentration of LYZ was successfully converted into optical fluorescent signals. In this manner, we established an immunofluorescent method for the detection of LYZ. The fluorescence switch efficiency (E_{switch}) was investigated [13]. In this study, E_{switch} is calculated by the equations below, in which F_0 and F_q are the fluorescence intensities of QDs-LYZ in the absence and presence of anti-LYZ-AuNPs, and F_r is the fluorescence of the system when free LYZ is present.

$$E_{switch} = E_q \times E_r \quad (1)$$

$$E_q = (F_0 - F_q)/F_0 \quad (2)$$

$$E_r = (F_r - F_q)/F_0 \quad (3)$$

E_q was calculated to be 0.359. E_r was calculated to be 0.180. Thus, the E_{switch} was 0.0646.

The fluorescence intensity of the system was measured under optimal conditions at different concentrations of LYZ, and the calibration curve was constructed according to the relationship between the LYZ concentration (C) and the corresponding fluorescence intensity change (ΔF). Fig. 3D illustrates the linear increase in the fluorescence intensity with increased concentrations of LYZ. The

linear range for LYZ was from 50 to 1000 ng/mL, and the standard regression equation was $\Delta F = 0.121\ C + 6.346$ (C= ng/mL), and the correlation coefficient $R^2 = 0.993$. The limit of detection (LOD) was defined by the equation, $LOD = 3S_0/K$, where S_0 is the standard deviation of blank measurements (n=11), and K is the slope of the calibration curve. In this equation, the LOD was 33.43 ng/mL.

The data for the linear range and LOD that was obtained by various methods of LYZ detection were collected and are presented in Table 1, which shows a comparison of the different methods. It can be seen from the table that the G-quadruplex luminescent method [11] had a relatively low LOD value and excellent specificity, but its detection range was narrow. The QD fluorescence quenching method [31] had a wider detection range. However, the LOD value was high and resulted in lower sensitivity. Furthermore, QDs conjugated with molecularly imprinted polymers require tedious operations and greater than 20 h. The gold nanorod heat-induced aggregation method [6] had good sensitivity with an aptamer. However, it required heating. The method proposed in this study had a relatively lower LOD and higher sensitivity and did not require extended analysis times, complex operations and expensive apparatus.

3.5 Anti-interference ability of the system

The influence of coexisting substances, such as Na^+, K^+, glucose, lactose, glycine, cysteine, glutathione, aspartic acid, L-serine, tyrosine, vitamin C, albumin, avidin and BSA, was investigated (Supplemental Data Table S1). The LYZ detection

concentration was 10^{-12} to 10^{-10} mol/L, and all concentration for the coexisting substances was significantly higher than the LYZ detection concentration. Many of the coexisting substances, such as ions, amino acids and proteins, had little influence on the determination of LYZ within a relative error of 5%, indicating that this method was resistant to interference by these substances.

3.6 Analytical performance

Table 2 displays the analysis of five synthetic samples. In real egg products, salts, amino acids, proteins, saccharides, vitamins and other substances are present. Therefore, in each synthetic sample, we selected salts, amino acids, proteins, saccharides and vitamins to simulate an actual sample and to assess interference in the method. Table 2 also shows that a certain concentration of the synthetic samples had little influence on the detection system. The strong interaction between LYZ and anti-LYZ might contribute to these results. Thus, the detection of LYZ exhibited minimal interference. The proposed method proved to be sensitive, simple and reliable.

3.7 Analysis of actual samples

To examine the applicability of this method, actual products (yolk powder and whole egg powder) were evaluated using this method. Egg powder samples were pretreated to remove high-abundance proteins. The concentration of LYZ in the food samples was determined using our experimental procedure. The egg white powder

sample contained 6.39 mg of LYZ per g of egg powder. The whole egg powder contained 3.49 mg of LYZ per g of egg powder. The content of LYZ in these egg powder samples was approximately equal to the standard value of LYZ concentration in eggs, namely, 3 mg of LYZ per mL of plain yolk. Thus, the method established in this study was suitable for the determination of LYZ concentrations in egg products.

4. Conclusions

This fluorescence switch LYZ detection method was based on specific interactions between QDs-LYZ and anti-LYZ-AuNPs, which rendered the detection more sensitive, rapid and selective. In the fluorescence switch system, LYZ in samples and QDs-LYZ combined with anti-LYZ-AuNPs competitively, thereby resulting in the recovery of fluorescence intensity from quenching QDs. Under optimal conditions, a linear calibration equation was obtained with a detection limit of 33.43 ng/mL. The fluorescence switch method established in this work was applied to the quantitative determination of LYZ in egg products. This study highlights the sensitive and selective detection of protein using a FRET fluorescence switch and specific molecular interactions.

Acknowledgments

This research was supported by the National Natural Science Foundation of China (No.31371810) and the Central University Basic Scientific Research Business Expenses Special Funds Project (2662015PY080).

References:

[1] L. Sheng, J. Wang, M. Huang, Q. Xu, M. Ma, The changes of secondary structures and properties of lysozyme along with the egg storage, International Journal of Biological Macromolecules. 92 (2016) 600-606.

[2] M. Schindler, Y. Assaf, N. Sharon, D.M. Chipman, Mechanism of lysozyme catalysis: role of ground-state strain in subsite D in hen egg-white and human lysozymes, Biochemistry. 16 (1977) 423-31.

[3] L.E. Smith, L.H. Mohr, M.A. Raftery, Mechanism for lysozyme-catalyzed hydrolysis, Journal of the American Chemical Society. 95 (1973) 7497-7500.

[4] Z.X. Cai, H.F. Yu, M.H. Ma, Determination of lysozyme at the nanogram level in food sample using Resonance Rayleigh-scattering method with Au nanoparticles as probe, Spectroc. Acta Pt. A-Molec. Biomolec. Spectr. 78 (2011) 1266-1271.

[5] R. Cegielska-Radziejewska, G. Lesnierowski, J. Kijowski, Antibacterial activity of hen egg white lysozyme modified by thermochemical technique, European Food Research and Technology. 228 (2009) 841-845.

[6] T.T. Moghadam, B. Ranjbar, Heat induced aggregation of gold nanorods for rapid visual detection of lysozyme, Talanta. 144 (2015) 778-787.

[7] P. Morsky, Turbidimetric determination of lysozyme with Micrococcus lysodeikticus cells: reexamination of reaction conditions, Analytical biochemistry. 128 (1983) 77-85.

[8] L. Pellegrino, A. Tirelli, A sensitive HPLC method to detect hen's egg white

lysozyme in milk and dairy products, International Dairy Journal. 10 (2000) 435-442.

[9] B. Kerkaert, F. Mestdagh, B. De Meulenaer, Detection of hen's egg white lysozyme in food: Comparison between a sensitive HPLC and a commercial ELISA method, Food Chem. 120 (2010) 580-584.

[10] P. Wu, X.P. Yan, Doped quantum dots for chemo/biosensing and bioimaging, Chem. Soc. Rev. 42 (2013) 5489-5521.

[11] L. Lu, W. Wang, M. Wang, T.-S. Kang, J.-J. Lu, X.-P. Chen, Q.-B. Han, C.-H. Leung, D.-L. Ma, A luminescent G-quadruplex-selective iridium(III) complex for the label-free detection of lysozyme, Journal of Materials Chemistry B. 4 (2016) 2407-2411.

[12] R. Zhang, W. Chen, Nitrogen-doped carbon quantum dots: Facile synthesis and application as a "turn-off' fluorescent probe for detection of Hg2+ ions, Biosensors & Bioelectronics. 55 (2014) 83-90.

[13] J. Wang, Y. Chang, P. Zhang, S.Q. Lie, P.F. Gao, C.Z. Huang, Cu2+-mediated fluorescence switching of gold nanoclusters for the selective detection of clioquinol, Analyst. 140 (2015) 8194-8200.

[14] M. Han, X. Gao, J.Z. Su, S. Nie, Quantum-dot-tagged microbeads for multiplexed optical coding of biomolecules, Nature Biotechnology. 19 (2001) 631-635.

[15] C. Ma, F. Zeng, L.F. Huang, S.Z. Wu, FRET-Based Ratiometric Detection System for Mercury Ions in Water with Polymeric Particles as Scaffolds, J. Phys. Chem. B. 115 (2011) 874-882.

[16] Q.-Y. Cai, J. Li, J. Ge, L. Zhang, Y.-L. Hu, Z.-H. Li, L.-B. Qu, A rapid fluorescence "switch-on" assay for glutathione detection by using carbon dots-MnO2 nanocomposites, Biosensors & Bioelectronics. 72 (2015) 31-36.

[17] N. Wanichacheva, O. Hanmeng, S. Kraithong, K. Sukrat, Dual optical Hg2+-selective sensing through FRET system of fluorescein and rhodamine B fluorophores, Journal of Photochemistry and Photobiology a-Chemistry. 278 (2014) 75-81.

[18] R. Xiao, H. Zhang, Y. Chi, Z. Feng, R. Xiao, Comparison of disinfection effect of egg surface by different treatment methods, Science & Technology of Food Industry. 34 (2013) 129-132.

[19] Q. Ma, X.G. Su, X.Y. Wang, Y. Wan, C.L. Wang, B. Yang, Q.H. Jin, Fluorescence resonance energy transfer in doubly-quantum dot labeled IgG system, Talanta. 67 (2005) 1029-1034.

[20] X. Wang, X.Q. Guo, Ultrasensitive Pb(2+) detection based on fluorescence resonance energy transfer (FRET) between quantum dots and gold nanoparticles, Analyst. 134 (2009) 1348-1354.

[21] J.J. Liu, Z.X. Shi, Y.C. Yu, R.Q. Yang, S.L. Zuo, Water-soluble multicolored fluorescent CdTe quantum dots: Synthesis and application for fingerprint developing, J. Colloid Interface Sci. 342 (2010) 278-282.

[22] B. Wang, X. Huang, M. Ma, Q. Shi, Z. Cai, A simple quantum dot-based fluoroimmunoassay method for selective capturing and rapid detection of Salmonella Enteritidis on eggs, Food Control. 35 (2014) 26-32.

[23] Y. Zhao, M. Ye, Q. Chao, N. Jia, Y. Ge, H. Shen, Simultaneous Detection of Multifood-Borne Pathogenic Bacteria Based on Functionalized Quantum Dots Coupled with Immunomagnetic Separation in Food Samples, Journal of Agricultural and Food Chemistry. 57 (2009) 517-524.

[24] M. Odabasia, R. Sayb, A. Denizli, Molecular imprinted particles for lysozyme purification, Materials Science and Engineering: C. 27 (2007) 90–99.

[25] A. Tankrathok, S. Daduang, R. Patramanon, Purification Process for the Preparation and Characterizations of Hen Egg White Ovalbumin, Lysozyme, Ovotransferrin, and Ovomucoid, Preparative Biochemistry & Biotechnology. 39 (2009) 380–399.

[26] H.L. Tao, S.H. Li, J.P. Li, Fluorescence Resonance Energy Transfer Between Quantum Dots of CdSe and CdTe and Its Application for Determination of Serum Prostate-Specific Antigen, Chinese Journal of Analytical Chemistry. 40 (2012) 224-229.

[27] K.M. Dorney, J.D. Baker, M. L. Edwards, Tangential Flow Filtration of Colloidal Silver Nanoparticles: A "Green" Laboratory Experiment for Chemistry and Engineering Students, Journal of Chemical Education. 91 (2014) 1044-1049.

[28]C. Ocaña, A. Hayat, R. Mishr, A novel electrochemical aptamer–antibody sandwich assay for lysozyme detection, Analyst. 140 (2015) 4148-4153.

[29]X. Cui, M. Liua, B.X. Li, Homogeneous fluorescence-based immunoassay via inner filter effect of gold nanoparticles on fluorescence of CdTe quantum dots, Analyst. 137 (2012) 3293-3299.

[30] X. Fu, K.L. Huang, S.Q. Liu, A rapid and universal bacteria-counting approach using CdSe/ZnS/SiO_2 composite nanoparticles as a fluorescence probe, Analytical and Bioanalytical Chemistry. 396 (2010) 1397-1404.

[31] X. Zhang, S. Yang, L. Sun, Surface-imprinted polymer coating l-cysteine-capped ZnS quantum dots for target protein specific recognition, Journal of Materials Science. 51 (2016) 6075-6085.

Figures and Tables

Scheme 1 Principle of the fluorescence switch control system.

Fig. 1 TEM images of QDs (A), QDs-LYZ (B), AuNPs (15.36 μg/mL) (C), QDs-LYZ-anti-LYZ-AuNPs (D) and the QDs-LYZ-anti-LYZ-AuNPs system with free LYZ (E).

Fig. 2 Fluorescence spectra of CdTe QDs (a), QDs-LYZ (b) and absorption spectra of AuNPs (c).

Fig. 3 Fluorescence spectra (A) and fluorescence intensity (B) of mixed system at different concentration of anti-LYZ-AuNPs. The concentrations of anti-LYZ-AuNPs from a to f are 0, 5, 10, 15, 20 and 25 μg/mL. The calculation is based on the concentration of AuNPs. (C) Changes in fluorescence spectra of the QDs-LYZ-anti-LYZ-AuNPs complex in the presence of different concentrations of LYZ. (D) Linear relationship between concentrations of LYZ and the changes in fluorescence intensity. The concentration of LYZ is from (a) to (h): 0, 50, 100, 200, 400, 600, 800 and 1000 ng/mL.

Scheme 1

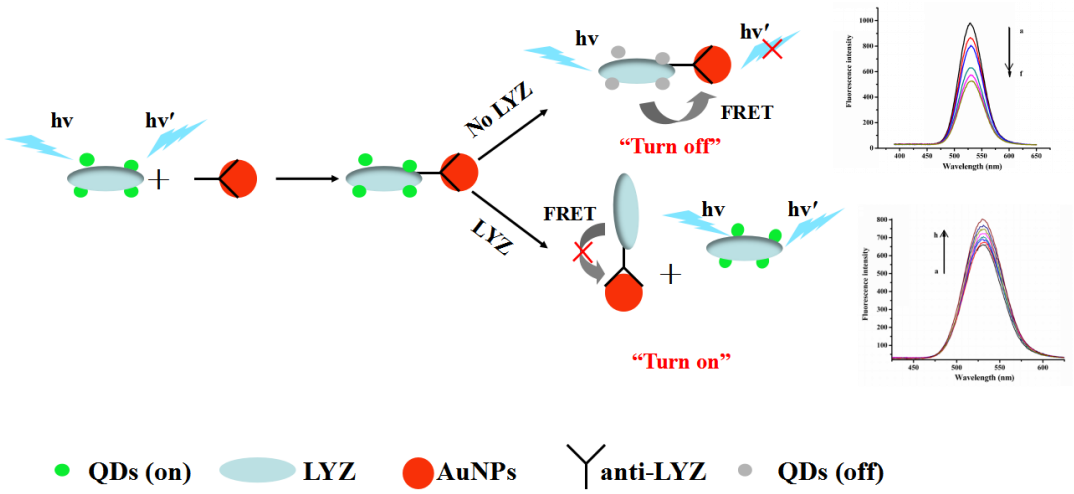
hv
hv′
No LYZ
LYZ
hv
hv′
FRET
“Turn off”
FRET
hv
hv′
“Turn on”
Wavelength (nm)
Wavelength (nm)
QDs (on)
LYZ
AuNPs
anti-LYZ
QDs (off)

Fig. 1

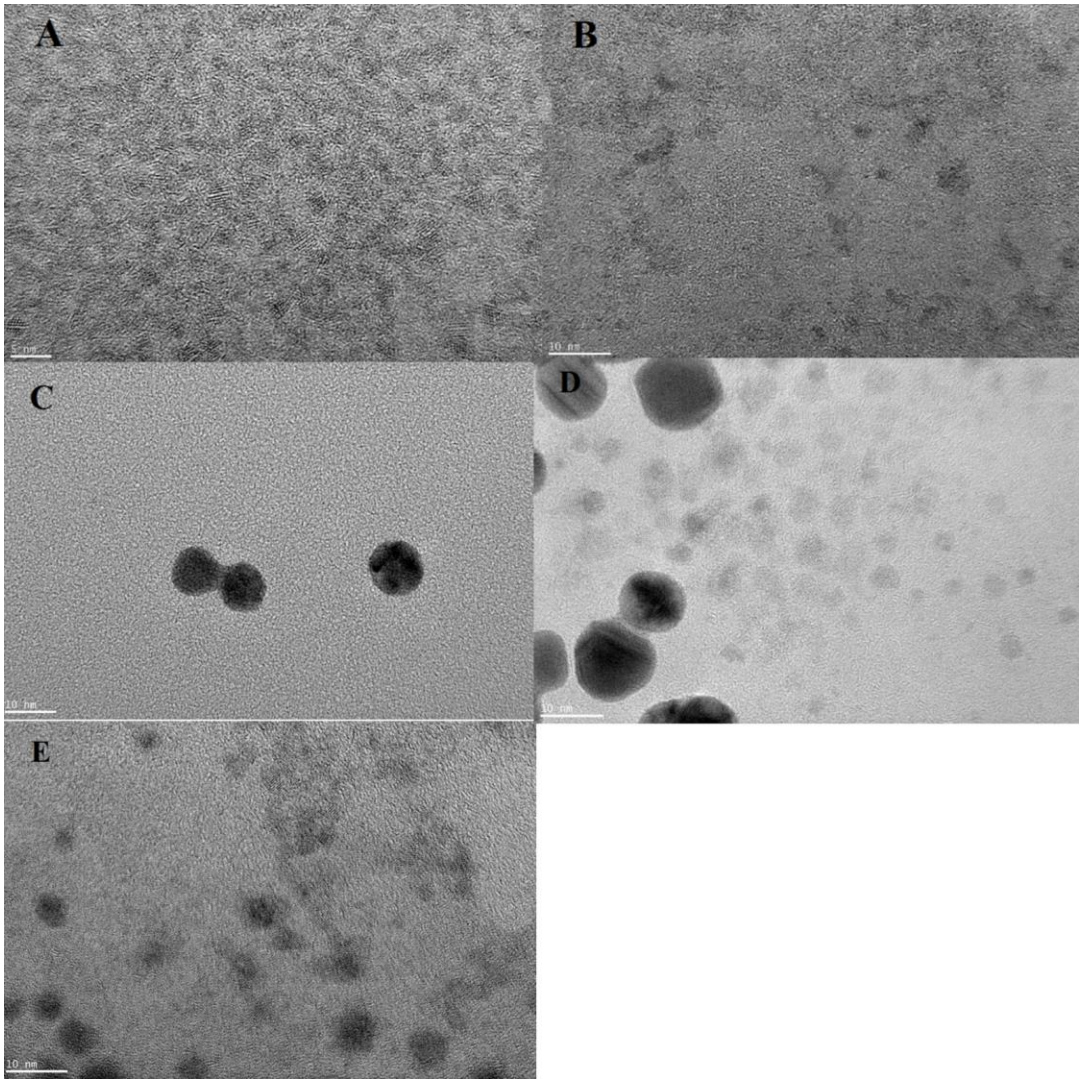

Fig. 2

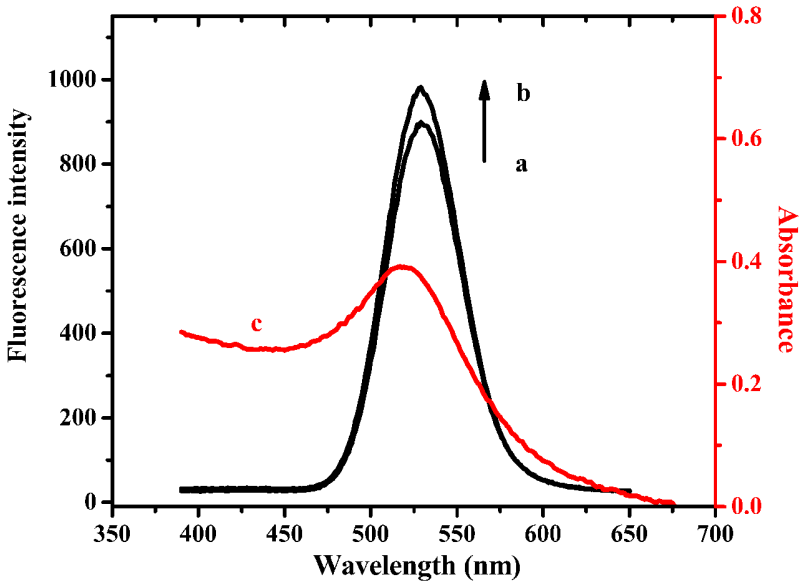
Fluorescence intensity
Absorbance
Wavelength (nm)
a
b
c
0
200
400
600
800
1000
0.0
0.2
0.4
0.6
0.8
350
400
450
500
550
600
650
700

Fig. 3

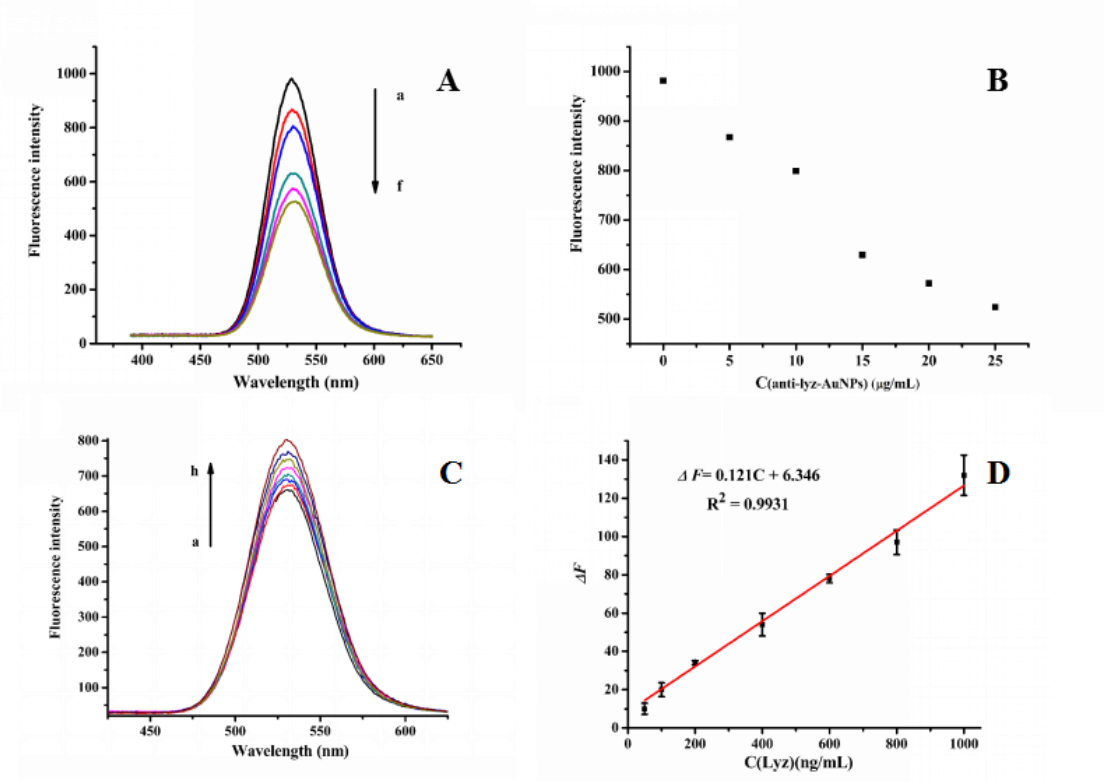
A
Fluorescence intensity
Wavelength (nm)
a
f
B
Fluorescence intensity
C(anti-lyz-AuNPs) (μg/mL)
C
Fluorescence intensity
Wavelength (nm)
h
a
D
ΔF
ΔF= 0.121C + 6.346
R2 = 0.9931
C(Lyz)(ng/mL)

Table 1 Comparison of the linear ranges and LODs for several methods for the determination of LYZ

Method	Linear range (ng/mL)	LOD (ng/mL)	Reference
Gold nanorods heat induced aggregation method	NM[a]	290	Moghadam et al., 2015
QDs fluorescence quenching method	1470-29400	370	Zhang et al., 2016
G-quadruplex luminescent method	29-735	29	Lu et al., 2016
This study	50-1000	33.43	

Note: NM[a] indicates no mention in the paper.

Table 2 Results for LYZ determination in synthetic samples

Synthesis sample	Main interferences（10^{-8} mol/L）	Change in fluorescence intensity (%)
1	Na^+ 1000，Tyrosine 2，Glucose 10，BSA 0.01，Vitamin C 1	+3.59
2	Na^+ 1000，L-serine 1，Lactose 100，Albumin 300，Glutathione1	-2.91
3	K^+ 1000，Glycine 10，Glucose 10，Avidin 147，Vitamin C 1	+4.52
4	K^+ 1000，Cysteine 2，Glucose 10，BSA 0.01，Vitamin C 1	+3.99
5	K^+ 1000，L-serine 1，Lactose 100，Avidin 147，Albumin 300	+2.66